Backwashable dynamic membrane made of anchored CNT on SiC microfiltration membranes applied to oil in water emulsion filtration

A. Poli, R. Sfeir, A. Ferreira Santos, M. Jacob, C. Batiot-Dupeyrat, B. Teychene

Initial submission date 31th may 2021

Revision 10th August 2021

Submission to: Separation and Purification Technology

Backwashable dynamic membrane made of anchored CNT on SiC microfiltration membranes applied to oil in water emulsion filtration.

A. Poli[1], R. Sfeir[1], A. Ferreira Santos[2], M. Jacob[3], P.Baldony-Andrey[3], C. Batiot-Dupeyrat[1], B.Teychene[1*]

1. IC2MP (UMR CNRS 7285), Université de Poitiers, 1 rue Marcel Doré, 86000 Poitiers, France.
2. UFPR, 1299 Rua XV de Novembro, 80060-000 Curitiba, Brazil.
3. TotalEnergies, Route de Bayonne, 64170 Lacq, France.

*Corresponding author : benoit.teychene@univ-poitiers.fr

Graphical abstract:

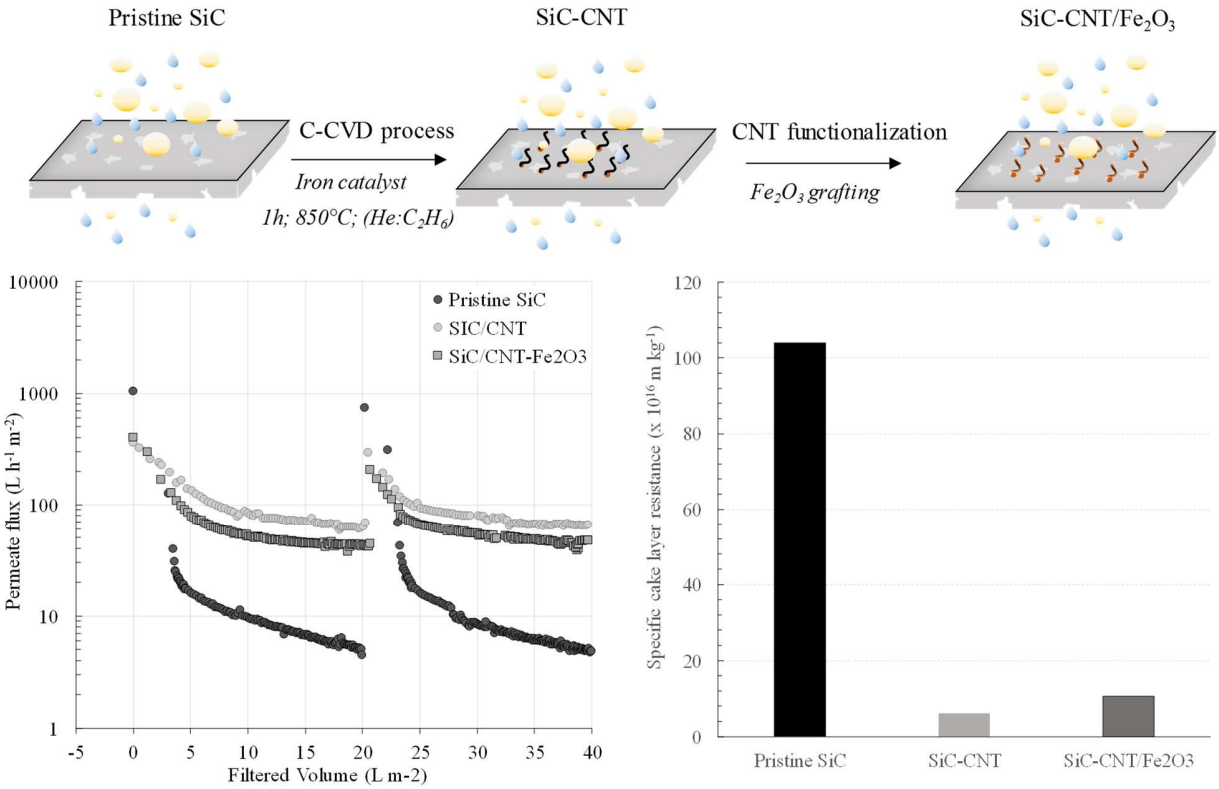

Highlights:

- SiC flat sheet membrane was employed for Oil in Water (O/W) emulsion filtration
- CNTs were successfully synthesized and functionalized at the SiC membrane surface
- Anchored CNTs improved permeate flux during O/W emulsion filtration
- CNTs and functionalized iron oxide CNTs acted as a dynamic membrane reducing the specific oil layer resistance without changing rejection values.

Abstract

Produced water is the highest liquid stream generated by the petroleum industry. It is most of the time saline water extracted with the petroleum or gas which contains less than 30 ppm of emulsified oil. SiC membrane material seems promising to treat such industrial wastewater and remove oil droplets but its development is still hindered by fouling phenomena. The present study investigates the filtration performances at lab-scale of a commercial flat sheet SiC membrane (55 cm^2) and the positive impact of CNTs synthesis by C-CVD process. The SiC pristine membrane exhibited a sharp flux decline of about 96 % for a low filtration volume (i;e : 4 L h^{-1} m^{-2} for 20 L m^{-2}). Results demonstrate that well anchored CNTs were successfully synthesized and functionalized on the SiC material. The hydrid SiC-CNTs materials showed permeate flux improvement with a higher permeate flux during O/W emulsion separation (i.e: 45 L h^{-1} m^{-2} for the same filtration conditions). Whatever the considered membrane, rejection values were excellent and above 90 %. Results also showed that the hydrophobic properties of SiC-CNTs membrane might be easily tuned by CNTs surface coating (i.e: iron oxide coating). Moreover, the synthesized CNTs were well anchored and might be backwashed keeping their positive impact on deposited oil. However, results emphasized that irreversible fouling tended to accumulate at the CNTs surface due to oil adsorption despite intensive chemical cleaning.

I. Introduction

Produced water (PW) is a by-product of oil and gas extraction. This oil-in-water (O/W) emulsion is the highest liquid stream generated by the petroleum industry with around 107 billion barrels generated worldwide (US EIA, 2017). Its composition is complex and includes many toxic compounds for the environment, such as alkyphenols and polyaromatic hydrocarbons inducing increasing regulations (Bakke et al., 2013). For instance, in 2020 in the north-east Atlantic Ocean, environmental impact at 500 m from oil platform should be reduced to nil, with an oil annual average discharge limit of 30 mg L^{-1} (OSPAR Convention). Many conventional techniques (sedimentation, flotation, hydrocyclones, nutshell filters) are suitable to demulsify PW with oil droplets larger than 20 µm [Othman et al .1988].

For sub-micron size droplets such techniques become hard to implement as predominant capture mechanisms change to interception, electrostatic forces and Brownian motion (Chen et al., 2016; Othman *et al.* 1988). For small droplets (<10 µm), it was demonstrated that coalescing fibrous filters and membrane filtration processes were found efficient to reach the required removal rates. For example, Agarwal *et al.* (2013) showed that high droplet removal might be achieved for multilayer fibrous filter with the highest fiber surface area facing the influent stream regardless its wettability. Moreover, Zsirai *et al.* (2018) found that cross flow ceramic microfiltration implemented at pilot-scale can sustain comparatively higher filtration fluxes and smaller foot print than flotation or granular filters.

One of the main drawbacks of membrane processes used for O/W emulsion separation relies on membrane fouling due to the accumulation of oil phase closed to the membrane surface. Therefore, improvement of membrane permeate flux and cleaning procedure efficiency during operation are key challenges. Due to their high chemical resistances inorganic membranes were

found more suitable for O/W emulsion filtration than organic materials. Most of reported works focused on ceramic membranes (consisting of Al_2O_3, TiO_2, ZrO_2, Mullite materials) separation of PW while only few studies investigated the efficiencies of silicon carbide (SiC) membranes[Rashad *et al.* (2021), Behroozi and Rostami-Ataabadi (2021)]. SiC membranes are quickly emerging as a promising material for harsh filtration environment due to their outstanding properties (chemical resistance, high water permeability and anti-fouling properties) [Eray *et al.* (2021)].

During O/W emulsion filtration, oil droplets are transported near the membrane surface by the convective permeation flow and then might accumulate on it [Behroozi and Rostami-Ataabadi (2021)]. As suggested by He *et al.* (2017) fouling induced by O/W occurs in three stages. According to the authors, the first stage (stage I) consisted of the accumulation of oil droplets leading to the formation of a continuous oil film at the membrane surface during stage II. During these two stages, the hydraulic resistance strongly increases depending on the filtered O/W and membrane characteristics. In Stage III, the permeate flux or the transmembrane pressure (TMP) enters into a pseudo-steady state in agreement to the critical pressure values calculated thanks to the Young Laplace equation using O/W and membrane characteristics (oil droplets, pore size, contact angle and oil surface tension) [Nazzal and Wiesner (1996)].

Based on reported results, changing the properties of oil film during filtration might be an interesting option to control membrane fouling. As stated by Shao *et al.* (2020), a movable micro/nanoscale rough structure might improve the removal of accumulated foulant and oil droplets at the membrane surface. Therefore, it is assumed that dynamic membranes (DM), consisting of an array of particles at the membrane surface, might control the surfactant and organic fouling in O/W emulsion filtration. Various materials used as DM (such as diatomite,

CNTs, MnO_2, Fe_2O_3…) were found to control and reduced fouling. Few study investigated DM for O/W emulsion filtration and reported results generally showed that the DM might control foulant deposition and improve flux recovery after membrane cleaning [Yang *et al.* (2011), Pan *et al.* (2012), Zhao *et al.* (2005), Lu *et al.* (2016)].

However, as recently pointed out by Anatharaman *et al.* (2020) several problems are related to DM: (i) irreproducibility during DM removal and deposition cycles and (ii) potential production during DM regeneration of concentrated effluents containing contaminants and DM materials (specifically when nanomaterials are used as DM). Therefore, an ideal DM might offer a good protection for the primary membrane and should be well anchored to the membrane surface in order to facilitate fouling layer cleaning without removing the DM layer. Such arrangement might be defined as "backwashable" DM.

The development of efficient, well anchored and "backwashable" DM is a key challenge for membrane widespread application. Among the different available technical choices, the synthesis of carbon nanotubes (CNTs) at the membrane surface by chemical vapor deposition (CVD) seems promising for such application. Indeed, CNTs might be anchored at the membrane surface making them sustainable through numerous filtration-cleaning cycles by avoiding the DM deposition cycles step. In addition, due to their hydrophobic character CNTs exhibit high affinity regarding oil phase through CH/π interactions and might promote oil droplet coalescence and rejection [Ajmani *et al.* (2012), Chen *et al.* (2012)].

Chen *et al.* (2012) pioneered the CNTs synthesis on inorganic membranes. Briefly, CNTs were grown onto/into a ceramic substrate impregnated with a metal catalyst (Ni or Fe) by CVD at 500-850°C. Later Tran *et al.* (2015) demonstrated the possibility to scale up the fabrication procedure to tubular commercial ceramic membranes. After CNTs synthesis, the hybrid

membrane material consists of an asymmetric hierarchical porous structure consisting of a thin CNTs grid at the membrane surface and within the membrane's pore volume [Tran *et al.* (2015)]. Specifically the CNTs grid might act as an anchored DM while the ceramic membrane might be considered as the primary membrane. Chen *et al.* (2016) further studied the separation performances of their new CNTs-Mullite membranes during O/W emulsion filtration. The results showed that the CNT-Mullite membranes outstand the pristine membrane performances with higher rejection and lower fouling tendency. Recently, Zhu *et al.* (2019) developed a CNT-Mullite hollow fiber membranes for high temperature O/W emulsion filtration. However, these previous studies were only conducted on homemade Mullite membranes making comparison with commercially available membrane materials difficult. Consequently, several works are still needed to develop CNTs-hybrid ceramic membranes with outstanding surface properties and exhibiting sustainable anti-fouling effect throughout cleaning-filtration cycles.

To this end the present study investigates the synthesis of a CNTs grid at the surface of a commercial SiC membranes in order to produce a DM that could be cleaned by backwash. Such membranes defined as "backwashable" DM, might offer antifouling properties over several filtration cycle without the need of deposition cycle. Moreover, modification of CNTs by iron oxide grafting was investigated in order to change the hydrophobic surface properties of the CNTs. Filtration performances of the aforementioned modifications were investigated at lab-scale (membrane surface area equals to 55 cm^2) through O/W emulsion (0.1% w/w) filtration in dead end mode.

2. Materials and methods

2.1 Membranes and lab-scale filtration pilot

SiC flat sheet membranes were purchased from Cembrane company (Denmark). The membranes are fully made of silicon carbide (SiC) displaying an active layer porosity of 0.1 µm and thickness of around 60 µm. According to the manufacturer the iso-electrical point is around 2.7.

The SiC membranes were cut into small pieces (L145×W3×T6 mm) having an effective surface area of 55 cm^2. The membrane pieces were glued between two teflon elements using epoxy glue (Araldite 2021, France). The membrane module was then inserted inside a homemade dead end filtration cell (Fig S1-a). The filtration cell exhibited a total volume of 110 mL.

Smaller membrane pieces (L30×W10mm) were used for preliminary surface modification experiments (C-CVD and CNT modifications, see section 2.4) as well for membrane characterization.

2.2 Filtration procedure

The dead end filtration cell was connected to a 5 L pressure vessel (Sartorius, France) to allow longer filtration time (Fig. S1-b). The transmembrane pressure (TMP) was provided by nitrogen gas source and was ranged from 0 – 1 bar. Pure water membrane permeability was determined using MilliQ water (18.2 MΩ). Three pressure steps were performed for a duration of 5 minutes each while the mass of the collected permeate was recorded every second by an electronic balance (VWR SE1202, France) recorded by a homemade LabVIEW program. The membrane permeate flux was calculated and corrected at 20°C thanks to Eq.1 and Eq.S1, respectively.

$$J_{20°C} = \frac{1}{S}\frac{dV}{dt} = Lp_{20°C}.\Delta P = \frac{\Delta P}{(\mu_{20°C}.R_m)} \qquad \text{Eq 1.}$$

Where, $J_{20°C}$ is the permeate flux corrected at 20°C in L h^{-1} m^{-2}; S is the membrane surface area (m^2); V and t are the filtered volume (in L) and time (in sec), respectively. $Lp_{20°C}$ is the membrane permeability at 20°C (L h^{-1} m^{-2} bar^{-1}). ΔP is the transmembrane pressure (in bar). $\mu_{20°C}$ is the water viscosity (in bar s) and R_m is the membrane hydraulic resistance (m^{-1}).

O/W emulsion dead end filtration test was performed at 0.2 bar for a total filtered volume equals to 110 mL (20 L m^{-2}). The permeate flux was recorded every 10 seconds and the permeate quality was evaluated at 2 and 18 L m^{-2}. The fouling propensity were evaluated in terms of flux decline ($J_{V=110\ mL}/J_{V=0}$) and the flux recovery rate was evaluated by comparing the initial permeate flux and the permeate flux obtained after a cleaning step.

Initial and final fouling mechanisms throughout the considered filtration cycle were evaluated thanks to the four empirical models developed by Hermia (Eq. S2-S6) using Rstudio software [Hermia (1982)]. The fouling model determination was based on the R^2-adjusted criteria and p-value.

The filtration experiment consisted of two cycles interspersed by a membrane backwash performed at 0.7 bar. In order to investigate the best cleaning conditions various solutions were investigated on the pristine membrane. The investigated cleaning solutions were: Pure water, NaOH (1 mol L^{-1}) and a sodium dodecyl sulfate/ethylenediaminetetraacetic acid solution 5 mM each (SDS/EDTA). The SDS ($C_{12}H_{25}NaO_4S$, purity ≥ 99%) was purchased from Sigma aldrich (France) and EDTA $C_{10}H_{14}N_2Na_2O_8.2H_2O$; purity > 99%) was purchased from VWR chemicals (France).

2.3 O/W preparation and characterization

Synthetic O/W emulsion was investigated in this study. SDS anionic surfactant (88 mg) corresponding to a surfactant to oil weight ratio of 1:10 were added to 1 L of MilliQ and were magnetically stirred until the SDS fully dissolved. Subsequently, 1 mL of Total Activa 5000 15W-40 diesel oil (density at 15°C of 0.888 $kg.m^{-3}$, API gravity of 28° and a dynamic viscosity at 40°C of 110 $mm^2.s^{-1}$) corresponding to an oil concentration of 0.1 % (v/v) were then added and mixed for 5 minutes at a speed of 21,000 RPM using a T18 digital Ultra Turrax mixer (IKA, Germany). Prior filtration, the O/W emulsion was left to stand for at least 1 h allowing the unstable large oil droplets to float leaving behind emulsified oil. Only the emulsified oil was used for filtration tests. The O/W emulsion was characterized in terms of non-purgeable organic carbon (NPOC) thanks to a TOC-$V_{CSH/CSN}$ SHIMADZU (Kyoto, Japan). The turbidity was measured using a WTW Turb 550 IR (WTW, France). Finally the droplets diameter was determined by a Zetasizer Nano ZS (Malvern; France).

The corresponding O/W emulsion exhibited average turbidity, NPOC values and oil droplets diameter equal to 908 +/- 78 NFU, 262 +/- 33 mg_C L^{-1} and 837 +/- 44 nm, respectively.

2.4 Membranes modification procedures

2.4.1 CNTs synthesis on SiC by C-CVD process

SiC membrane piece was first deep coated in an ultrasonic bath (300 W) for 1 h with 1.5 Fe wt% iron (III) chloride aqueous solution ($FeCl_3.6H_20$ sigma Aldrich, France). Then the impregnated membrane was dried in an oven at 100°C for 1 h and regularly flipped *(approximately every 20 min)* to maintain a homogeneous distribution of catalyst at the surface. The membrane was

then calcined into a furnace at 350°C for 2 h where the iron (III) ions were transformed into iron (III) oxide. Finally, the investigated sample was inserted into a quartz reactor where the C-CVD takes place under a 1:1 ratio He:H_2 mix (120 mL min^{-1}). The gas mixture was preheated in a first reactor at 200°C and reached the second reactor heated to 600°C and kept for 1 hour allowing the reduction of the iron (III) oxide into active Fe(0) catalyst which promotes the CNTs growth during the CVD process [Tran *et al.* (2015)]. The temperature in the quartz reactor was then increased up to 850°C and the gas inlet was switched to a He:C_2H_6 blend (120 mL min^{-1}) for 1 h. The ethane is thus cracked and deposited on the membrane surface as carbon nanotubes (single and multiwall) as well as amorphous carbon [Venegoni *et al.* (2002)]. The membrane sample was left to cool down inside the reactor in an inert atmosphere (He: H_2 1:1 with a total flowrate of 2 mL min^{-1}). Finally, in order to remove unanchored synthesized carbonaceous materials at the membrane surface several 30 minutes sonication cycles in MilliQ water were performed until nothing came off the membrane. The described C-CVD process was first performed on the small membrane pieces (L30×W10mm) for membrane characterisation and then applied to larger membrane samples for O/W filtration tests.

2.4.2 Fabrication of the SiC-CNT/Fe_2O_3 membranes

In order to change the CNTs surface properties (i.e: Hydrophobicity), the synthesized SiC-CNT membrane was first oxidized and finally covered with Fe_2O_3. This method was based on the work of Ihsanullah et al (2016). The SiC-CNT membrane was oxidized in a nitric (0.1 M) and sulfuric (0.05 M) mixture solution (3:1 v/v) refluxed and kept for 2 h after boiling. This allows the oxidation of the carbon nanotubes at the membrane surface. The membranes were then immersed in a 0.5 Fe wt% iron (III) chloride solution, sonicated for 1 h and then dried at 100°C for 1 h with

continuous flipping. Finally, the membranes were calcined in a furnace at 350°C for 2 h to provide iron (III) oxide coating onto the membrane and CNTs surface.

2.5 Membrane characterization

2.5.1 CNTs structures and C-CVD yield

The carbon material synthesis yield (C wt%) was determined using thermal analysis (TGA/DSC) thanks to a Q series Q600-0471 analyzer (TA Instruments, USA) after crushing samples into powder using a mortar. The synthesis yield of stable material (undergone the ultrasonic treatment, see section 2.4.1) was evaluated according to the weight loss obtained from around 30 mg of initial mass in the 600-700°C range specific to carbon structures [Pang *et al.* (1993)].

Carbon structure defects were assessed by Raman spectroscopy operated at 532 nm using a confocal Labram HR800UV (Horiba Jobin Ivon, Japan). The quality of the carbon structure surface layer was evaluated thanks to the I_D/I_G ratio. The Raman intensity of D-band (I_D) refers to the defects of the graphitic structures while the G-band intensity (I_G) corresponds to the orientation degree of the CNTs [Antunes *et al.* (2007)]. The D and G bands are observed in the 1300-1350 cm^{-1} and the 1570-1600 cm^{-1} ranges, respectively. The I_D/I_G ratio was calculated using pseudo-Voigt function, a combination Lorentzian and Gaussian deconvolution functions [Merlen *et al.* (2017)].

Scanning electron microscopy pictures (SEM) were obtained on a JSM-7900F (JEOL, Japan) coupled with an energy-dispersive X-ray spectroscopy analyzer (EDS).

2.5.2 Underwater contact angle (UWCA)

The impact of SiC membrane modification on wettability was evaluated through underwater contact angle measurements (UWCA). Tests were conducted in the captive bubble mode since the investigated membrane was too porous to sustain droplets in air. Oil droplets of around 6 µL sampled from Total Activa 5000 15W-40 were released at the membrane surface being submerged under 88 mg L^{-1} sodium dodecyl sulfate (SDS) anionic surfactant solution diluted in MilliQ water (20°C). Motor oil surface tension was measured as 24 mN m^{-1}. UWCA was measured using a drop shape analyzer DSA25 (Kruss, Germany) and measurements were done in triplicate on every investigated sample. A measurement example is provided in figure S2.

3. Results and discussion

3.1 Membranes characterization

Figure 1 reports the SEM images of the three investigated membranes. As shown on Fig.1-a (upper part), the pristine SiC membrane exhibits an active layer thickness equals to 60 µm supported by large SiC particles. As revealed by the figure 1.a (bottom part) the porous structure of the SiC membranes active layer consists of SiC particles with a diameter centred at around 1 µm. The TGA analysis demonstrates that the SiC membrane was stable up to 1000°C (figure 2-a).

The figure 1-b shows the active layer of the SiC-CNT membrane. As shown on Fig 1-b (right) the synthesized CNTs were grown at the membrane surface and within the membrane porous structure. The CNT diameter was equal to 137 +/- 10 nm. As emphasized by the SEM image obtained in compo mode, the catalyst iron particles remained at the membrane surface (white dots on Fig1-b, left). The presence of iron element was confirmed by EDS analysis (figure 1-d).

As shown on figure 2-a, the synthesized CNT temperature decomposition was ranged from 450 to 650°C. TGA analysis reveals that 2.3% w/w of stable carbonaceous materials were synthesized according to the C-CVD conditions employed in this study (Table 1). In addition, the Raman spectra of the SiC-CNT membrane (Fig. 2-b) shows a classical CNT footprint with two sharp bands centred around 1350 and 1580 cm^{-1} corresponding to the D and G bands, respectively. The corresponding I_D/I_G ratio equals to 1.08 suggests that MWCNTs were mainly present on the investigated sample [Merlen *et al.* (2017)].

The SEM picture of the SiC-CNT/Fe_2O_3 membrane was reported on figure 1-c. Some CNT are still visible while the majority seems to be embedded within the Fe_2O_3 coating layer. As

emphasized by SEM picture in compo mode (figure 1-c, left) the Fe_2O_3 coating covered most of the anchored CNT as white tubes are clearly visible. This was confirmed by EDS mapping as reported in Figure S3. Iron element was mostly found on MWCNTs (green colour). In addition, it can be seen that the iron oxide coating on CNTs changed the surface of the synthesized layer. The carbonaceous material synthesis yield was equal to 2.7%w/w which is similar of the SiC-CNT membrane (Table 1). This observation emphasises that CNTs oxidation process prior Fe_2O_3 grafting did not impact the amount of anchored CNTs. Indeed, it is important to note that only well attached CNT remained on the membrane after the intensive ultrasonic treatment performed subsequently to the C-CVD process (see section 2.4.1).

The EDS analysis performed on the three membranes (Fig. 1-d) indicates that the SiC membrane consists of pure SiC material. The SiC-CNT membrane showed a similar spectrum with two additional bands related to the iron catalyst and oxygen elements. The EDS spectra of the SiC-CNT/Fe_2O_3 revealed two intense bands related to the presence of Iron and Oxygen which was confirmed by the EDS pictures given in Fig.S3.

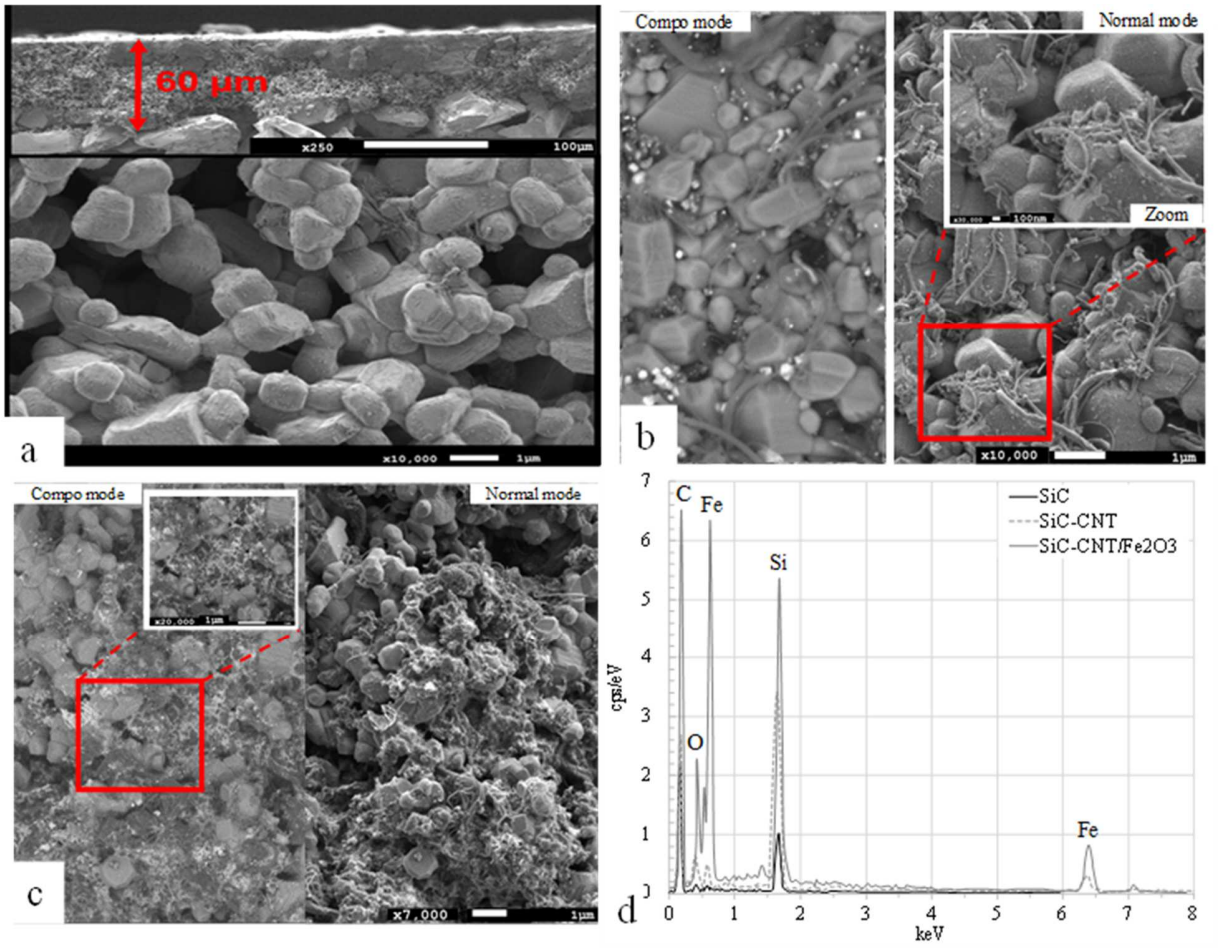

Figure 1: SEM images of (a) the pristine SiC (*top: cross section; bottom: active layer*), (b) SiC-CNT active layer (*left: compo mode; right normal mode*), (c) SiC-CNT/Fe_2O_3 (*left: compo mode; right normal mode*), (d) EDS spectra of the three membranes.

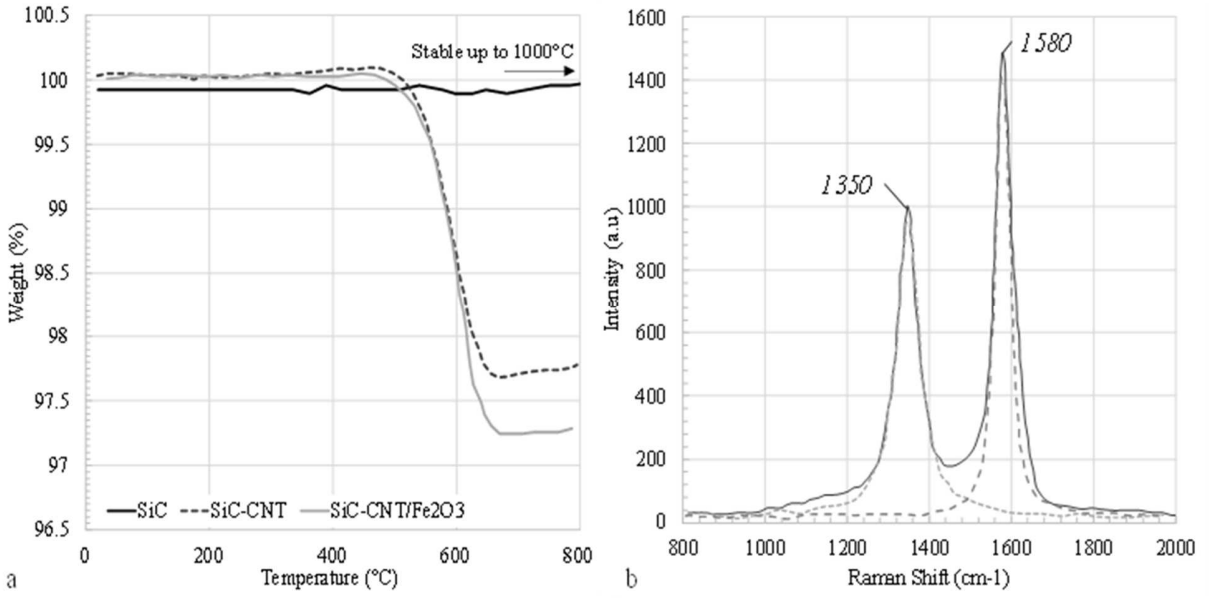

Figure 2: (a) TGA analysis of the three membranes. (b) Raman spectra of CNT synthesized on SiC membrane (SiC-CNT sample), dotted lines represent the peaks deconvolution.

Table 1: Membranes properties

Membranes	UWCA	C yield (%)	Permeability (L h^{-1} m^{-2} bar^{-1})
Pristine SiC	138.8 +/- 6°	-	5505 +/- 127
SiC-CNT	57 +/-3°	2.3	1791 +/- 67
SiC-CNT/Fe2O3	104+/-10°	2.7	3256 +/- 111

As reported in table 1, the SiC membrane is highly hydrophilic with an UWCA equals to 138.8 +/- 6°. In contrast the MWCNTs synthesis on the membrane strongly decreased the

hydrophobic properties of the SiC membrane with an UWCA equals to 57 +/- 3°. As expected, the additional Fe_2O_3 coating reduced the hydrophobic character of MWCNTs and the resulting UWCA of the modified membrane was equal to 104 +/- 10°. Therefore, the additional treatments including CNTs oxidation prior to Fe_2O_3 grafting increased the CNTs hydrophilicity [Ihsanullah *et al.* (2016)].

As previously reported by Cumming *et al.* (2000), the UWCA might strongly influence the filtration performances during O/W emulsion filtration. Indeed, a change in hydrophilicity might influence the critical pressure above which oil droplets penetrate the membrane. As depicted in Fig. 3-a, the critical pressure (predicted from Eq. S8) of the pristine membrane increases with the oil droplet diameter. As an example, at a critical pressure equal to 0.2 bar the oil droplet diameter is equal to 70 nm which is lower than the membrane pore size. Oppositely, the critical pressure calculation on the SiC-CNT could not be done as this membrane is considered as totally wetted by oil (UWCA < 90°) [Darvishzadeh *et al.* (2018)]. Interestingly, calculation done on the SiC-CNT/Fe_2O_3 membrane demonstrates that the modified membrane led to lower critical pressure than the pristine SiC with an oil droplet diameter equals to 200 nm at 0.2 bar. However, it is important to note that the critical pressure calculation was done with a constant membrane pore size equals to 0.1 µm and potential pore size reduction or change in surface roughness due to CNT synthesis was not taken into account.

3.2 Filtration performances of hybrid inorganic materials.

As reported in table 1 the pristine SiC membrane permeability was equal to 5505 +/- 127 L h^{-1} m^{-2} bar^{-1}. In contrast the pure water permeabilities of the SiC-CNT and SiC-CNT/Fe_2O_3 membranes were much lower than the primary SiC membrane and were equal to 1791 +/- 67 and 3256 +/- 111 L h^{-1} m^{-2} bar^{-1}, respectively. The CNTs synthesis on the SiC material strongly reduced membranes' permeability due to pore blockage and hydrophobic character. The higher pure water flux of the SiC-CNT/Fe_2O_3 membrane compared to the SiC-CNT is attributed to the increase of the UWCA due to Fe_2O_3 coating and CNT oxidation.

Filtration results and permeate qualities during O/W emulsion filtration were reported on figure 3-b and table 2, respectively. The filtration test consisted of two cycles at 0.2 bar in dead end mode with high oil contents (262 +/- 33 mg_C L^{-1}, see section 2.3). As shown on figure 3-b, the initial permeate flux obtained for the pristine SiC membrane was equal to 1050 L h^{-1} m^{-2} which is relevant with the initial membrane's permeability. As shown, the SiC membrane exhibited a rapid flux decline of 96% for a low filtered volume (4 L m^{-2}). Finally, the permeate flux decreased to 4.5 L h^{-1} m^{-2} at the end of the first filtration cycle (20 L m^{-2}). The rapid flux decline observed for the SiC membrane was attributed to a rapid obstruction of the large pore observed at the membrane surface (figure 1-a). As reported by Zsirai *et al.* (2016), SiC membrane are prone to fouling due to more open pores than other ceramic membranes (i.e : TiO_2).

According to the filtration model described in sup data (Eq.S2- S6), the permeate flux decline was well modelled by the cake layer built up for filtered volume ranged from 5 to 20 L m^{-2} (Table S1). This confirms that the small oil droplets approaching the membrane surface might rapidly block the open membranes' pores (for low filtered volume) and accumulate over already deposited oil subsequently leading to the built up of a cake layer. Such observation was also

relevant with oil droplets mean diameter in the feed (837 +/- 44 nm) larger than the membrane pore size.

The rejection values in terms of NPOC and turbidity were high and equal initially to 94.8 % (12.6 mg_C L-1) and 96.6 % (27 NFU), respectively. At the end of the first filtration cycle, rejection values slightly decreased to 78.5 % and 95.1 % for NPOC and turbidity, respectively. The oil droplet diameters in permeate were equal to 176 +/- 16 and 121 +/- 12 nm at the beginning and end of the filtration test, respectively. These values are similar to the membrane pore size but higher than the values predicted by the critical pressure calculation (70 nm at 0.2 bar, figure 3-a). These results discrepancy might be related to membrane roughness and large pore diameters observed on the SEM picture (figure 1-a) which are not taken into account for critical pressure calculation (Eq.S8).

Various membrane cleaning strategies were investigated in order to obtain the best permeate flux recovery. As shown in figure 3-c, MilliQ water backwash (at 0.7 bar 300 mL) recovered only 45% of the initial permeability, indicating that the motor oil and its high concentration used for dead end filtration test led to strong irreversible fouling. Consequently, chemical cleaning was needed to recover the membrane's permeability.

The permeability obtained after NaOH (1 mol L^{-1}) backwash at 0.7 bar (300 mL) increased up to 3090 L h^{-1} m^{-2} bar^{-1} corresponding to a permeate flux recovery of 56 %. Finally, a maximum of 91 % of permeate flux recovery was obtained with a SDS/EDTA backwash at 0.7 bar for 109 L m^{-2} (600 mL). Consequently, the SDS/EDTA backwash was chosen to recover the membrane flux after O/W emulsion filtration whatever the considered membranes.

Table 2: Permeate qualities obtained during the dead end filtration cycles.

		Cycle 1				Cycle 2			
Membranes	Filtered volume ($L\ m^{-2}$)	Turbidity in NFU (Rejection %)	NPOC ($mg\ L^{-1}$) (Rejection %)	Droplet diameters (nm)	Specific resistance ($m\ kg^{-1}$)	Turbidity in NFU (Rejection %)	NPOC ($mg\ L^{-1}$) (Rejection %)	Droplet diameters (nm)	Specific resistance ($m\ kg^{-1}$)
Pristine SiC	2	26.6 (96.6%)	12.6 (94.8%)	176 +/-16	$9.6\ 10^{17}$	2.0 (99.8%)	15.1 (93.5%)	90+/-1	$1.1\ 10^{18}$
	18	38.3 (95.1%)	52.6 (78.5%)	120 +/-12		81.3 (90.8%)	66.5 (71.4%)	200+/-17	
SiC-CNT	2	2.2 (99.8%)	16.4 (92.2%)	101+/-33	$7.5\ 10^{16}$	4.8 (99.5%)	14.9 (94.3%)	123+/-2	$4.6\ 10^{16}$
	18	24.4 (97.6 %)	45.9 (78.2%)	165+/-10		48.8 (94.8%)	54.1 (79.4%)	163+/-5	
SiC-CNT/Fe_2O_3	2	2.2 (99.8%)	20.4 (92.3%)	141+/-8	$1.2\ 10^{17}$	5.8 (99.3%)	12.4 (95.4%)	165+/-6	$9.6\ 10^{16}$
	18	51.8 (94.7%)	55.9 (78.9%)	233+/-24		63.4 (92.7%)	64.8 (76.2%)	167+/-7	

The initial permeate flux of the second filtration cycle equals to 740 L h^{-1} m^{-2} which is lower than the theoretical value obtained from membrane permeability measurement (i.e: 5064 L h^{-1} m^{-2} bar^{-1}x 0.2 bar = 1013 L h^{-1} m^{-2}). This indicates a rapid fouling of O/W emulsion at the beginning of the filtration test. Similar to the first filtration cycle, the permeate flux strongly decrease of about 94% for a filtered volume of 4 L m^{-2}. The permeate flux finally reached 4 L h^{-1} m^{-2} at the end of the filtration cycle. Permeate quality was once again excellent with turbidity rejection higher than 90 % throughout the filtration test and NPOC values equal to 93.5 % and 72 % at the beginning and the end of the filtration test, respectively. The oil droplet diameter reached 200+/-17 nm at the end of the filtration test. The lower rejection values and higher droplet diameter compared to the first cycle might be attributed to change in membrane properties such as an decrease of the UWCA of the pristine SiC membrane despite membrane chemical cleaning.

The permeate flux recovery after the SDS/ETDA backwash was about 91 % (4991 L h^{-1} m^{-2} bar^{-1}) indicating that irreversible fouling might not be totally removed by chemical backwash. Similar to the first filtration cycle, the fouling mechanisms was determined as cake layer built up throughout the filtration cycle (Table S1). This suggests that irreversible fouling might be due to the irreversible adsorption of oil over the membrane surface.

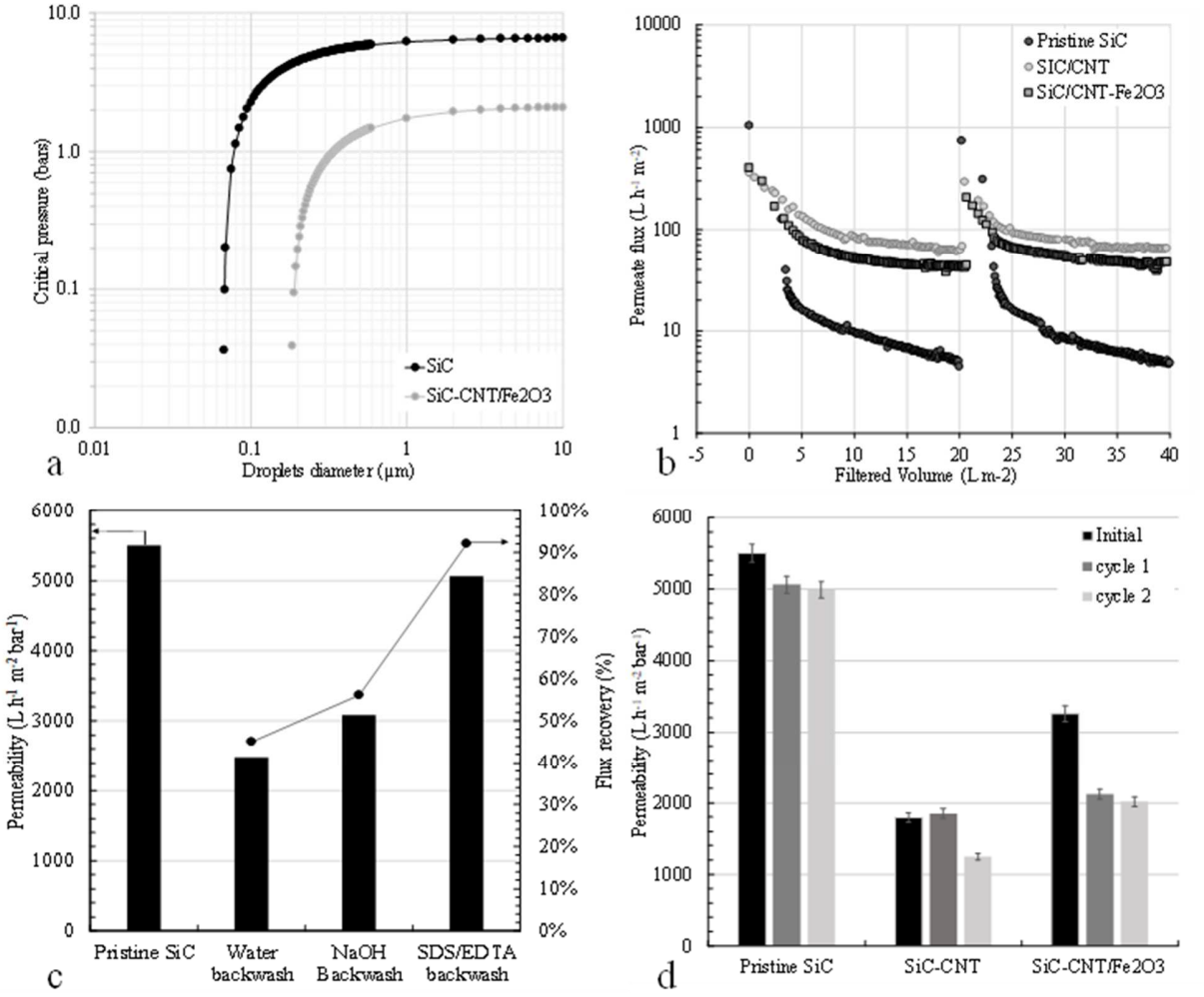

Figure 3: (a) Critical pressure versus oil droplets diameter (pore size : 0.1 µm); (b) Permeate flux decline during O/W emulsion dead end filtration 2 cycles at 200 mBar (Log scale); (c) Improvement of membrane cleaning on pristine SiC membrane; (d) Permeability after SDS/EDTA backwash.

The SiC-CNT membrane showed an initial permeate flux of about 358 L h^{-1} m^{-2} and sharply decreased to 132 L h^{-1} m^{-2} for a filtered volume equals to 5 L m^{-2}. At the end of the filtration cycle

(20 L m^{-2}) the permeate flux was higher than the pristine SiC membrane and was equal to 60 L h^{-1} m^{-2}.

Similar to the pristine SiC membrane, rejection values were high (Table 2). The droplets diameters were equal in the permeate to 101+/-33 and 165+/-10 nm at the beginning and end of the first cycle, respectively. Over the different Hermia's models, the filtration mechanism was determined as cake layer built up (Table S1).

A total permeate flux recovery was obtained after SDS/EDTA backwash done at the end of the first filtration cycle (Figure 3-d). In addition, the initial permeate flux observed for the second filtration cycle was lower and was equal to 300 L h^{-1} m^{-2} despite the total flux recovery. This observation shows that the oil phase quickly adsorbs on the CNT conducting to a sharp decrease of the initial permeate flux.

At the end of the second filtration cycle, the permeate flux of the SiC-CNT membrane was equal to 65 L h^{-1} m^{-2}. As reported on table 2, the SiC-CNT membrane showed higher rejection values compared to the pristine SiC membrane regarding the second filtration cycle (with 79% rejection in term of NPOC). These higher values might be due to a potential adsorption of oil droplet on the CNTs surface or a better sieving effect due to lower pore size diameter due to CNT growth (Figure 1-b).

The flux decline during the second cycle was modelled by the cake layer mechanism. The final SDS/EDTA backwash was not able to totally remove fouling and only 60% of the initial permeability was recovered. This indicates that despite intensive chemical cleaning the oil droplets tend to accumulate at the membrane and/or CNT surface due to hydrophobic interactions.

The SiC-CNT/Fe_2O_3 membrane showed a lower initial permeate flux compared to pristine SiC membrane and was equal to 397 L h^{-1} m^{-2} at the beginning of the first filtration cycle and stabilized at around 47 L h^{-1} m^{-2} for a filtered volume of 20 L m^{-2}. The flux recovery was about 65% indicating that SDS/EDTA backwash was not enough efficient to remove irreversible oil fouling on the SiC-CNT/Fe_2O_3 membrane. Consequently, the initial permeate flux at the beginning of the second cycle was the lowest value of the three membranes and was equal to 200 L h^{-1} m^{-2}.

However, despite this low value the permeate flux stabilized at around 45 L h^{-1} m^{-2} at the end of the second filtration cycle. Similar flux recovery of 60% was observed as for the first filtration cycle. Moreover, the SiC-CNT/Fe_2O_3 membrane still exhibited higher permeability equals to 2016 +- 69 L h^{-1} m^{-2} bar^{-1} compared to the SiC-CNT membrane (Fig. 3-d). Results reported on table 2 showed that the permeate rejection values for the SiC-CNT/Fe_2O_3 were closed to the results obtained for the SiC-CNT membrane. The cake layer model was once again found to better describe fouling mechanism on the SiC-CNT/Fe_2O_3 whatever the filtration cycle or filtered volume.

These results showed that the SiC membranes are strongly fouled by the investigated O/W emulsion and that the best cleaning conditions were obtained for the SDS/ETDA backwash. The membrane modification strategy was found to reduce membrane permeability due to higher hydrophobicity and potential pore blockage due to the CNTs growth but led to higher permeate flux compared to virgin membrane during O/W emulsion filtration. However, results emphasized that irreversible fouling tends to accumulate on modified membranes and efficient cleaning strategy should be investigated.

In terms of membrane fouling mechanisms, the strong initial permeate flux decline was attributed to pore blocking mechanisms but most of the filtration curve might be modelled by cake layer mechanism. To this end, the specific cake layer resistances obtained on all filtration tests were calculated and reported in table 2. As high rejection values were observed, the specific cake layer resistances were calculated using the feed O/W emulsion NPOC values (262 +/- 33 mg_C L^{-1}).

As reported in table 2, the highest specific resistances were obtained for the SiC membrane and the mean value equals to 1.0 +/- 0.1 10^{18} m kg^{-1} over the two cycles. In contrast, the specific resistances obtained on the modified membranes are much lower and the mean values equal to 6.0 +/- 2.0 10^{16} and 1.0 +/- 0.2 10^{17} m kg^{-1} for the SiC-CNT and SiC-CNT/Fe_2O_3 membranes, respectively.

The strong reduction of the oil fouling layer at the membrane surface might be attributed to the CNTs at the membrane surface. The anchored CNTs at the membrane surface might structure the fouling layer and also adsorb oil droplets leading to higher final permeate flux. However, modification of CNT by Fe_2O_3 coating does not led to lower specific resistance due to a potential repulsion of oil and Fe_2O_3 layer.

4. Conclusion

Modification of SiC microfiltration membrane materials (surface area ~ 55 cm^2) was investigated in this study. To this end, the CNTs were successfully synthesized thanks to C-CVD process at 850°C using iron catalyst. According to the C-CVD conditions employed, around 2.3 % w/w of carbonaceous materials mostly consisting of MWCNTs were synthesized. In addition, it was demonstrated that anchored CNTs might be easily functionalized with iron oxide coating.

It was also demonstrated that the synthesized CNTs reduced the pure water membrane permeability and that the membranes' hydrophobicity might be controlled depending on the CNTs surface properties. The permeability reduction was attributed to the hydrophobic characters of the CNTs and potential pore blockage.

Filtration results of highly concentrated O/W with small oil droplet diameters (< 1 µm) showed that the pristine SiC exhibited sharp permeate flux decline of about 94 % but excellent rejection values in terms of NPOC and turbidity. The final permeate flux was improved whatever the considered modifications (CNTs or CNTs/Fe_2O_3) without changing the excellent rejection performances (above 90%).

In addition, whatever the considered membrane the cake layer built up was found to well described the permeate flux decline trends. Consequently, it was demonstrated that the synthesized CNTs at the membrane's surface strongly reduces the specific cake layer resistance of the oil fouling layer. Such observation was attributed to the potential adsorption of oil at the CNTs surface structuring the oil cake layer. Finally, membrane backwash using SDS/EDTA solution was found to efficiently clean the pristine SiC membrane but reported results suggested an irreversible fouling accumulates at the CNTs surface. This suggests that better cleaning strategy has to be investigated for the SiC-CNTs membrane using for example the specific electronic properties of the CNTs (i.e: microwaves). Also, it is suggested that the CNTs layer is embedded into a rigid matrix of Fe_2O_3 which reduces the backwash efficiency. Consequently, the amount of metal oxide grafted on CNTs should be investigated carefully in order improve hydrophilicity and keeping backwash efficiency.

Further studies are still needed to develop efficient anchored dynamic membranes in order to improve membranes' anti-fouling resistance during O/W emulsion filtration.

References:

Agarwal S., Von Arnim V., Stegmaier T., Planck H. & Agarwal, A. Effect of Fibrous Coalescer Geometry and Operating Conditions on Emulsion Separation. Ind. Eng. Chem. Res. **52**, 13164–13170 (2013)

Ajmani G.S., Goodwin D., Marsh K., Fairbrother D.H., Schwab K.J., Jacangelo J.G., Huang H., Modification of low pressure membranes with carbon nanotube layers for fouling control, Water Res. **46**, 5645–5654 (2012).

Anantharaman A., Chun Y., Hua T., Chew J.W., Wang R., Pre-deposited dynamic membrane filtration – A review, Water Res., **173**, 115558 (2020).

Antunes E.F., Lobo A.O., Corat E.J., Trava-Airoldi V.J., Influence of diameter in the Raman spectra of aligned multi-walled carbon nanotubes, Carbon. **45**, 913–921, (2007).

Bakke, T., Klungsøyr, J. & Sanni, S. Environmental impacts of produced water and drilling waste discharges from the Norwegian offshore petroleum industry. Marine Env. Res. **92**, 154–169 (2013).

Behroozi A.H, Rostami Ataabadi M. Improvement in microfiltration process of oily wastewater: A comprehensive review over two decades, J. Env. Chem. Eng., **9** (1), 104981 (2021).

Chen X., Hong L., Xu Y., Ong Z.W., Ceramic Pore Channels with Inducted Carbon Nanotubes for Removing Oil from Water, ACS Appl. Mater. Interfaces. **4**, 1909–1918, (2012).

Chen, X., Lim, J. F., Xu, Y. & Hong, L. Operating conditions and feed composition on filtering emulsified oil using ceramic-hybrid membrane. Ceram. Int. 42, 17101–17109 (2016).

Cumming I.W., Holdich R.G., Smith I.D. The rejection of oil by microfiltration of a stabilized kerosene/water emulsion. J. Membr. Sci., **169**, 147-155, (2000).

Darvishzadeh T., Bhattarai B., Priezjev N.V. The critical pressure for microfiltration of oil-in-water emulsions using slotted-pore membranes, J. Membr. Sci., **563**, 610-616, (2018).

Eray E., CandelarioV.M., Boffa V., Safafar H., Østedgaard-Munck D.M., Zahrtmann N., Kadrispahic H., Jørgensen M.K. A roadmap for the development and applications of silicon carbide membranes for liquid filtration: Recent advancements, challenges, and perspectives, Chem. Eng. J., **414**, 128826 (2021).

Hermia J., Constant pressure blocking filtration laws—application to power-law non-newtonian fluids, Trans. Inst. Chem. Eng. **60**, 183−187, (1982).

Ihsanullah, Al Amer A.M., Laoui T., Abbas A., Al-Aqeeli N., Patel F., Khraisheh M., Ali Atieh M., Hilal N., Fabrication and antifouling behaviour of a carbon nanotube membrane, Materials & Design, **89**, 549-558, (2016).

Lu D., Cheng W., Zhang T., Lu X., Liu Q., Jiang J., Ma J. Hydrophilic Fe2O3 dynamic membrane mitigating fouling of support ceramic membrane in ultrafiltration of oil/water emulsion. Sep. Purif. Technol., **165**, 1-9, (2016).

Merlen A., Buijnsters J.G., Pardanaud C., A Guide to and Review of the Use of Multiwavelength Raman Spectroscopy for Characterizing Defective Aromatic Carbon Solids: from Graphene to Amorphous Carbons, Coatings. **7**, 153, (2017).

Nazzal F.F., Wiesner M.R.. Microfiltration of oil-in-water emulsions. Water Environ. Res., **68** 1187-1192, (1996).

OSPAR convention Convention for the Protection of the Marine Environment of the North-East Atlantic, (Paris 22 Sept. 1992).

Othman F. M., Fahim M. A., Jeffreys G. V., Mumford C. J. Prediction of Predominant Mechanisms in the Separation of Secondary Dispersions in a Fibrous Bed. J Dispers Sci Technol, **9**, 91–113 (1988)

Pan Y., Wang T., Sun H., Wang W. Preparation and application of titanium dioxide dynamic membranes in microfiltration of oil-in-water emulsions. Sep. Purif. Technol., **89**, 78-83, (2012).

Pang L.S.K., Saxby J.D., Chatfield S.P., Thermogravimetric analysis of carbon nanotubes and nanoparticles, J. Phys. Chem. **97**, 6941–6942, (1993).

Rashad O., Logesh G., Sabu U., Balasubramanian M. A novel monolithic mullite microfiltration membrane for oil-in-water emulsion separation, J. Membr. Sci., **620**, 118857 (2021).

Shao S., Liu Y., Shi D., Qing W., Fu W., Li J., Fang Z., Chen Y., Control of organic and surfactant fouling using dynamic membranes in the separation of oil-in-water emulsions, J. Colloid Interface Sci., **560**, 787-794, (2020).

Tran D.T., Thieffry G., Jacob M., Batiot-Dupeyrat C., Teychene B., Modification of tubular ceramic membranes with carbon nanotubes using catalytic chemical vapor deposition, Water Sci. Technol., 72, 1404–1410, (2015).

US EIA, 2017, U.S. Energy Information Administration (www.eia.gov).

Venegoni D., Serp P., Feurer R., Kihn Y., Vahlas C., Kalck P., Parametric study for the growth of carbon nanotubes by catalytic chemical vapor deposition in a fluidized bed reactor, Carbon. 40, 1799–1807, (2002).

Yang T., Ma Z.-F., Yang Q.-Y. Formation and performance of Kaolin/MnO2 bi-layer composite dynamic membrane for oily wastewater treatment: Effect of solution conditions. Desalination, 270 (1–3), 50-56, (2011).

Zhao Y., Tan Y., Wong F.-S., Fane A., Xu N. Formation of dynamic membranes for oily water separation by crossflow filtration. Sep. Purif. Technol., 44 (3), 212-220, (2005),

Zhengwang He, Daniel J. Miller, Sirirat Kasemset, Donald R. Paul, Benny D. Freeman, The effect of permeate flux on membrane fouling during microfiltration of oily water, J. Membr. Sci., **525**, 25-34 (2017).

Zhu L., Chen M., Dong Y., Tang C.Y., Huang A., Li L. A low-cost mullite-titania composite ceramic hollow fiber microfiltration membrane for highly efficient separation of oil-in-water emulsion. Water Res. **90**, 277-285, (2016).

Zsirai T., Al-Jaml A.K., Qiblawey H., Al-Marri M., Ahmed A., Bach S., Watson S., Judd S.J. Ceramic membrane filtration of produced water: impact of membrane module. Separ. Purif. Technol., 165, 214-221, (2016).

Zsirai T., Qiblawey H., Buzatu P., Al-Marri M., Judd, S. J. Cleaning of ceramic membranes for produced water filtration. J. Petrol. Sci. Eng., **166**, 283–289 (2018).